

# Effect of Important Physical and Geometrical Parameters on the Dynamic Response of Thick Composite Plates with Smart Attached Mass

**Alireza Pourmoayed\***

Department of Mechanical Engineering,  
University of Khatamul-Anbiya Air Defense, Iran  
E-mail: pourmoayed@mut.ac.ir

\*Corresponding author

**Keramat Malekzadeh Fard, Naser Zolghadr**

Department of Structural Analysis and Simulation, Aerospace research institute, University of MalekAshtar, Iran  
E-mail: kmalekzadeh@mut.ac.ir, naser.zolghadr@gmail.com

**Received: 9 September 2019, Revised: 18 November 2019, Accepted: 9 December 2019**

**Abstract:** In this research, the effect of different structural parameters on the dynamic behaviour of a thick plate with a smart attached mass, which is a mass embedded with the Shape Memory Alloy (SMA) fibers were investigated. The results showed that the inherent stiffness of the smart attached mass and the localized stiffness due to the effect of SMA fibers both play a significant role in the dynamic behaviour of the plate, and ignoring either of these parameters results in a considerable change in the system responses. The size and position of the smart attached mass were also found to be of particular importance, since the effect of the weight of SMA and attached mass and the forces induced by SMA transformation all have significant and sometimes conflicting effects on the system vibrations. The results also showed that the changes in the system parameters, and particularly the characteristics of the SMA fibers such as activation temperature, pre-strain, and volume fraction, result in the appearance of dynamic responses that cannot be neglected.

**Keywords:** Attached Mass, Free Vibrations, Higher-Order Theory, Mode Shape, Plate, Shape Memory Composites

**Reference:** Pourmoayed, A., Malekzadeh Fard, K., and Zolghadr, N., "Effect of Important Physical and Geometrical Parameters on the Dynamic Response of Thick Composite Plates with Smart Attached Mass", Int J of Advanced Design and Manufacturing Technology, Vol. 12/No. 4, 2019, pp. 67–81.

**Biographical notes:** **Alireza Pourmoayed** received his PhD in Airspace Engineering from Malek-Ashtar University of Technology in 2017. He is Assistant Professor of Mechanical engineering at the University of Khatamul-Anbiya Air Defense, Tehran, Iran. His current research interest includes Dynamic, Vibration and Buckling of structures. **Keramat Malekzadeh Fard** received his PhD in Mechanical Engineering from University of K. N. Toosi in 2005. He is currently Professor at the Department of Mechanical Engineering, Malek-Ashtar University of Technology, Tehran, Iran. **Naser Zolghadr** received his MSc from Malek-Ashtar University of Technology.

## 1 INTRODUCTION

The importance of dynamic behavior of structures in all venues of the industry has encouraged constant research on new materials that may contribute to the improvement of this behavior. Given the unique behavior of Shape Memory Alloys (SMAs), they have found exponentially increasing applications in various fields of engineering. Hence, the behavior of these materials in interaction with other structural components is worthy of research. The unique features that make SMAs a viable option for many engineering applications include high damping, adaptive responses, shape memory, and super elasticity. Due to their wide application in industry, analysis of the effect of different characteristics of SMA and attached mass on the vibration behavior of thick plates with SMA-containing attached mass can be an interesting subject of research. There are various theories to model a plate for further analysis.

The Classical Laminated-Plate Theory (CLPT), which is the basis of the plate analysis, ignores the effects of out-of-plane stresses and strains and cannot be relied upon to serve as a comprehensive theory, as it brings about cross-sectional warping that is often too large to be ignored, especially in thick plates. Yang et al. [1] extended the Reissner and Mindlin's First-Order Shear-Deformation Theory (FSDT) to laminated plates. Nevertheless, the simplifying assumptions made in classical and first-order theories have a high rate of error, especially in thick plates. The Higher-Order Shear-Deformation Theory (HOST), which includes a realistic parabolic variation of transverse shear stress along the laminate thickness and warping of the cross-section, is of great use for the analysis of plate problems, especially those with higher thicknesses. Kant et al. [2] were the first to provide a finite element formulation for the higher order bending theory. This theory incorporates the three-dimensional Hook's law and the effect of transverse vertical strain as well as transverse shear deformations.

Later, Reddy [3] proposed a higher order theory using a displacement field with cubic variations along thickness. This theory was then used by Reddy and Fan [4] to obtain closed-form solutions for the natural frequencies of elastic plates and by Khadir [5-6] to analyze the free vibrations of laminated plates. Kato [7-8] conducted extensive research on the dynamic behavior of homogeneous and laminated shells. Kant et al. [9] studied the free vibration characteristics of simply supported laminated cross-ply composite and sandwich shell panels by the use of several higher order theories and described the effects of vertical and transverse shear stresses and strains. Since the distribution of interlaminar shear stress over thickness is significantly influenced by the heterogeneity of the laminate, for

composites in which laminates of high and low moduli are stacked together, a significant warping can be expected.

In regard to the effect of attached mass, there have been many studies on the beams and rods that carry uniformly distributed masses. However, only a few studies have investigated the ones carrying distributed masses. Gorman [10] solved the problem of free vibration of a point supported plate with attached mass using the superposition principle. Rossi [11] solved the problem of vibration of a fully clamped plate with attached mass by combining the boundary element method with the finite element method. Kopmaz and Telli [12] studied the free vibration of a plate carrying a distributed mass using a mathematical model. They used the Galerkin method to solve the derived partial differential equation, and then obtained eigenvectors and frequencies accordingly. Wang [13] analyzed the free vibration of a simply supported rectangular plate carrying a distributed mass using the Rayleigh-Ritz method. Alibeiglu et al. [14] solved the problem of free vibration of a simply supported single-layer composite with a distributed attached mass using the Hamilton principle and a double Fourier series. Malekzadeh et al. [15] investigated the effect of attached mass on the vibration of a thick plate with the plate stiffness taken into consideration, and obtained significant results using the higher-order theory.

Among the studies on the effects of SMAs on the structure, only a few works have discussed the free vibrations of the plate with the effects of SMAs or smart sandwich panels taken into consideration. Stakovich et al. [16] studied the effect of heat on the first natural frequency and the effect of SMAs on the critical buckling temperature of SMA-containing composite plate, and showed that an increase in pre-strain and temperature results in an increase in the critical buckling temperature of the plate. Lu et al. [17] studied the vibrational properties of the SMA-containing composite beam with different boundary conditions. Using the finite element method, they showed that increasing the temperature of the pre-tensioned SMA increases the natural frequency. They reported that to increase the damping ratio, the fibers must be embedded in the composite without pre-tension.

Alimozaffari et al. [18] showed that the embedding an SMA into the laminates of a hybrid composite increases the natural frequency of the system. Zhang et al. [19] investigated the variations of natural frequency of an SMA-containing composite plate by the use of finite element method, and showed that adding SMA fibers and increasing the temperature increases the frequency of the system. Park et al. [20] examined the vibrational behavior of an SMA-containing composite plate in the post-buckling state using the finite element method and first-order shear-deformation theory. Their numerical

results showed that if we increase the SMA volume fraction and pre-strain, the natural frequency in the pre-buckling state will initially increase, but with the plate's thermal deflection gradually dominating the recovery stress, the frequency will decrease until buckling occurs. In addition, the natural frequency of an SMA-containing plate is always lower than the natural frequency of the same plate without SMA (at the reference temperature). This is because of the plate's increased weight and decreased thermal deflection due to the presence of SMA.

In a dynamic mechanical analysis conducted by Kingni et al. [21], they investigated the stiffness and vibrational properties of SMA-containing composite beams. This analysis showed that the addition of SMA affects the properties that depend on the vibrational temperature and dynamic mechanical characteristics, thus leading to reduced natural frequency. Zhang studied the SMA-containing composite beams under thermal and mechanical loads. This study showed that the compressive recovery stresses dominating the heat-induced tensile stresses leads to reduced natural frequency of the beam. Hariri et al. [23] investigated the variations of natural frequency of SMA-containing composite structures.

In this study, the governing equations were derived through a strain energy perturbation analysis and solved by the Rayleigh-Ritz analytical method. The results showed a slight decrease in the natural frequency of the system after the stimulation of SMA. Shokuhfar et al. [24] analyzed and optimized a hybrid composite plate under low velocity impact. They reported that after the symmetrical placement of tensioned SMA in different laminae at a temperature below the reference temperature, one can generate compressive stress by applying heat up to the activation temperature. Finally, they used the Navier's analytical method for dynamic analysis of the above plate. Hisham Hamed Ibrahim et al. at the University of Seoul studied the aero-thermo-mechanical characteristics of an SMA-containing composite plate. For this purpose, the finite element model was used to examine the static and dynamic behavior of the plate under the combined effect of thermal, mechanical and aerodynamic loads. They showed that in the pre-buckling region, as temperature increases, the natural frequency initially increases, but the thermal and aerodynamic loads gradually dominate the SMA-induced recovery stress and the natural frequency starts to decrease.

Yauko et al. [26] studied the effect of SMAs on the buckling of a composite plate using the finite element method. This study showed that the tensile recovery stress induced by the SMA pre-strain increases the buckling load and, consequently, the natural frequency of the system. Malekzadeh et al. [27] studied the free vibration response of SMA-containing composite plates.

In this study, the effects of geometric, physical, and material properties on the response of the composite plate were investigated. The first order shear deformation theory was used to derive the governing equations for the simply supported hybrid composite plate, which were then solved using the Navier method. For the first time in this research, the dynamic behavior of a thick plate that contains both Shape Memory Alloy (SMA) and a smart flexible attached mass was studied. The local distributed stiffness of attached mass was considered in dynamic simulation of the plate, simultaneously. In addition to the effects of different parameters such as activation temperature, pre-strain, and volume fraction were investigated. The results showed that these parameters are important and cannot be neglected.

## 2 THEORETICAL FORMULATION

### 2.1. Geometric Description

Figure 1 illustrates a thick plate of uniform thickness with a distributed attached mass on its upper surface. The Cartesian coordinates are represented by  $(X, Y, Z)$ , where  $X$  and  $Y$  are positioned in the mid-plane of the plate, and  $Z$  is normal to these axes according to the right-hand rule.

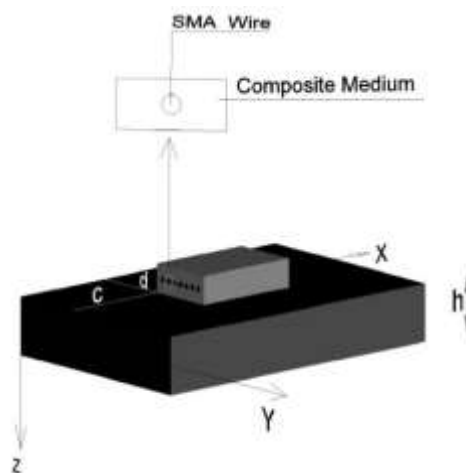


Fig. 1 Diagram of thick composite plate.

### 2.2. Displacement Field

In this study, we use the 12-variable displacement field proposed by Garg and Kant [9]. This displacement field can give better approximations of the plate state than CLPD and FSDT (particularly for thick plates), does not require shear correction factor, and can provide a more accurate representation of the interlaminar stress distribution. These features give this field an advantage over other higher-order displacement fields, especially for thick plates.

With the extension of displacements to the cubic term in the thickness coordinates, the following equations are derived:

$$\begin{cases} U = \sum_{i=0}^3 z^i u_i & , & V = \sum_{i=0}^3 z^i v_i \\ W = \sum_{i=0}^3 z^i w_i \end{cases} \quad (1)$$

Where, W, V, and U, are the displacement components of a general point in the plate. The terms  $(u_1, v_1, w_1)$ ,  $(u_2, v_2, w_2)$  and  $(u_3, v_3, w_3)$  are the functions defined in the mid-plane as follows:

$$\begin{cases} u_1 = \left(\frac{\partial u}{\partial z}\right)_{z=0} & , & v_1 = \left(\frac{\partial v}{\partial z}\right)_{z=0} & , & w_1 = \left(\frac{\partial w}{\partial z}\right)_{z=0} \\ 2u_2 = \left(\frac{\partial^2 u}{\partial z^2}\right)_{z=0} & , & 2v_2 = \left(\frac{\partial^2 v}{\partial z^2}\right)_{z=0} & , & 2w_2 = \left(\frac{\partial^2 w}{\partial z^2}\right)_{z=0} \\ 6u_3 = \left(\frac{\partial^3 u}{\partial z^3}\right)_{z=0} & , & 6v_3 = \left(\frac{\partial^3 v}{\partial z^3}\right)_{z=0} & , & 6w_3 = \left(\frac{\partial^3 w}{\partial z^3}\right)_{z=0} \end{cases} \quad (2)$$

Where,  $u_1$  and  $v_1$  represent the rotation of the reference plane normal vector around the X and Y axes, and the functions  $w_1, u_2, v_2, w_2, u_3, v_3, w_3$  are the high order terms of Taylor series expansion and represent the high order modes of deformation in cross-section.

### 2.3. Plate Kinematics

The shear and normal linear strains in the Cartesian coordinate system are defined as follows (M.H.Sadd, 1993):

$$\begin{cases} \gamma_{xy} = \frac{\partial U}{\partial y} + \frac{\partial V}{\partial x} & , & \epsilon_Y = \frac{\partial V}{\partial y} & \epsilon_x = \frac{\partial U}{\partial x} \\ \epsilon_z = \frac{\partial W}{\partial z} & , & \gamma_{yz} = \frac{\partial V}{\partial z} + \frac{\partial W}{\partial y} & \gamma_{xz} = \frac{\partial U}{\partial z} + \frac{\partial W}{\partial x} \end{cases} \quad (3)$$

Substituting “Eq. (1) into Eq. (3)” gives the linear strains in terms of displacements in the mid-plane of the plate. Assuming the main material axes as (1, 2, 3) and lamina axes as (x, y, z), the stress-strain relations are obtained as follows:

$$\{\sigma_{ij}\}^L = [C_{ij}]^L \{\epsilon_{ij}\}^L \quad (4)$$

Where, C components are as given in (A.K.Garg, R.K.Khare, T.Kant, 2006). Transforming the constitutive relations from the lamina axes (1, 2, 3) to the reference axes results in the following equation:

$$\sigma = Q \epsilon \quad (5)$$

Where, the components of the matrix Q are the reduced elastic constants of the orthotropic material in the L-th lamina. Integration of “Eq. (5)” with respect to plate thickness gives:

$$\bar{\sigma} = D \bar{\epsilon} \quad (6)$$

$$\begin{cases} \bar{\sigma} = \begin{Bmatrix} N_x, N_y, N_{xy}, N_x^*, N_y^*, N_{xy}^*, N_z, N_z^*, M_x, M_y, M_{xy} \end{Bmatrix} \\ \bar{\epsilon} = \begin{Bmatrix} \epsilon_{x0}, \epsilon_{y0}, \epsilon_{xy0}, \epsilon_{x0}^*, \epsilon_{y0}^*, \epsilon_{xy0}^*, \epsilon_{z0}, \epsilon_{z0}^*, X_x, X_y, X_{xy} \end{Bmatrix} \end{cases} \quad (7)$$

And D is defined as:

$$D = \begin{bmatrix} D_F & 0 \\ 0 & D_S \end{bmatrix} \quad (8)$$

The components of the matrix D are available in (J.N.Reddy, 2004). Therefore, the stress resultant components for N laminae are defined as:

$$\begin{cases} \begin{bmatrix} N_{xx} & N_{xx}^* & M_{xx} & M_{xx}^* \\ N_{yy} & N_{yy}^* & M_{yy} & M_{yy}^* \\ N_{zz} & N_{zz}^* & M_{zz} & 0 \\ N_{xy} & N_{xy}^* & M_{xy} & M_{xy}^* \\ N_{yx} & N_{yx}^* & M_{yx} & M_{yx}^* \end{bmatrix} \\ = \sum_{L=1}^N \int_{Z_L}^{Z_{L+1}} \begin{Bmatrix} \sigma_{xx} \\ \sigma_{yy} \\ \sigma_{zz} \\ \tau_{xy} \\ \tau_{yx} \end{Bmatrix} \{1, z, z^2, z^3\} dz \\ \begin{bmatrix} Q_x & Q_x^* & S_x & S_x^* \\ Q_y & Q_y^* & S_y & S_y^* \end{bmatrix} \\ = \sum_{L=1}^N \int_{Z_L}^{Z_{L+1}} \begin{Bmatrix} \tau_{xz} \\ \tau_{yz} \end{Bmatrix} \{1, z, z^2, z^3\} dz \end{cases} \quad (9)$$

### 2.4. Equations of Motion

The Hamilton principle is used to define the equations of motion in terms of displacement (“Eq. (1)”) and strain-displacement field (“Eqs. (2) and (3)”). The analytical form is expressed as follows:

$$\int_0^T \delta L dt \equiv \int_0^T [\delta K - (\delta U - \delta V)] dt = 0 \quad (10)$$

Where,  $\delta K$  is the kinetic energy,  $\delta U$  is the strain energy, and  $\delta V$  is the potential energy due to the applied loads, each of which can be expanded using “Eqs. (1) to (3)”. The kinetic energy variations are expressed as follows:

$$\delta k = \int_v \rho (\dot{U} \delta U + \dot{V} \delta V + \dot{W} \delta W) dv \quad (11)$$

Where,  $\rho$  is the mass density of the plate. After integration with respect to time T, the above equation transforms into:

$$\int_0^T \delta K dt = - \int_0^T \left[ \int_v \rho (\dot{U} \delta U + \dot{V} \delta V + \dot{W} \delta W) dv \right] dt + \int_v \rho (\dot{U} \delta U + \dot{V} \delta V + \dot{W} \delta W) \Big|_{t=t_0}^{t=T} dv \quad (12)$$

Setting the initial condition equal to zero results in the elimination of the second term. The most important part of obtaining the equations of motion is deriving the strain energy variation:

$$\begin{aligned} \delta U &= \int_V \sigma_{ij} \delta \varepsilon_{ij} dv \\ &= \int_{h/2}^{h/2} \sigma_{ij} \delta \varepsilon_{ij} A_1 A_2 dx dy dz \quad i, j = 1, 2, 3 \end{aligned} \quad (13)$$

Where,  $\sigma_{ij}$  and  $\varepsilon_{ij}$  are the stress and strain components, and the integration is made over the area of the mid-plane of the plate. As shown in “Fig. 2”, to add a smart attached mass, its energies must be added to the original system.

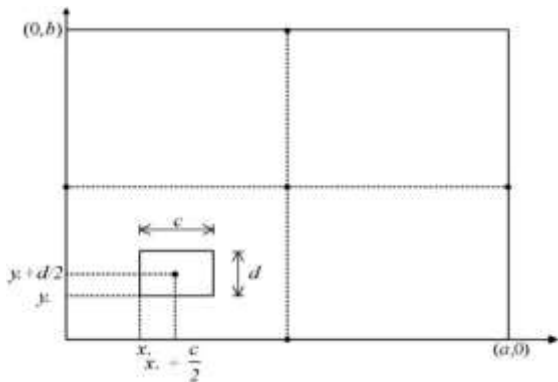


Fig. 2 Position of the SMA-containing attached mass.

It should be noted that these energies, which are associated with the attached mass, are only added to the surface where the attached mass is located. It is assumed that the attached mass does not prevent the plate from bending. In other words, the attached mass can take the form of the region of the plate on which it is positioned. Using the Heaviside functions, the following equations can be derived for the effect of the attached mass location:

$$\begin{aligned} K_{total} &= K_{plate} + H(x, y, x_0, y_0, c, d) K_{attached\ mass} \\ U_{total} &= U_{plate} + H(x, y, x_0, y_0, c, d) U_{attached\ mass} \end{aligned} \quad (14)$$

Where,  $x_0$  and  $y_0$  are the coordinates of the point on the attached mass that is closest to the origin,  $c$  and  $d$  are the width and length of the attached mass (see “Fig. 2”), and  $H$  is a combination of Heaviside functions that is introduced by Koppmaz (Koppmaz O, 2002) as follows:

$$\begin{aligned} H(x, y, x_0, y_0, c, d) &= [\hat{H}(x - x_0) \hat{H}(x - x_0 - c) * \\ &[\hat{H}(y - y_0) - \hat{H}(y - y_0 - d)]] \end{aligned} \quad (15)$$

Where,  $\hat{H}$  is the Heaviside function. The effect of  $H$  is expressed as follows:

$$\int_0^b \int_0^a H f(x, y) dx dy = \int_{y_0}^{y_0+d} \int_{x_0}^{x_0+c} f(x, y) dx dy \quad (16)$$

Integration of the kinetic energy variations with respect to time gives:

$$\begin{aligned} &\int_0^T \delta K_{total} dt \\ &= - \int_0^T \left[ \int_V \rho (\ddot{U}_1 \delta U + \ddot{V}_1 \delta V + \ddot{W}_1 \delta W) dv \right. \\ &\quad \left. + H \int_{\bar{V}} \bar{\rho} (\ddot{U}_1 \delta U + \ddot{V}_1 \delta V + \ddot{W}_1 \delta W) d\bar{v} \right] dt \end{aligned} \quad (17)$$

Where,  $\bar{v}$  and  $\bar{\rho}$  represent the volume and density of the attached mass, respectively. The strain energy variations are given by:

$$\delta U_{total} = \int_V \sigma_{ij} \varepsilon_{ij} dv + H \int_{\bar{V}} \bar{\sigma}_{ij} \bar{\varepsilon}_{ij} d\bar{v} \quad (18)$$

There are two ways for modeling the effect of SMA components on the structures: Active Property Tuning (APT) and Active Strain Energy Tuning (ASET). In the APT, structural stiffness is realized using the super elasticity of the embedded SMA or the variations of its elastic modulus with the temperature. In the ASET, the SMA elements, which are first placed under the strain (before embedding), are heated to produce a large recovery stress in the structure. In the present work, SMA is applied using the ASET technique. Since the effect of SMA is analyzed as an external load, the variations of potential energy should be reconsidered. In accordance with the method used in (S.Yao Kuo, L.C.Shiau , K.H.Chen, 2009), it is assumed that there is no thermal transfer between the attached mass and the SMA, and the micro-mechanic properties of SMA are ignored. According to (S.Yao Kuo, L.C.Shiau , K.H.Chen, 2009),  $N^r$ , i.e. the recovery force applied on the attached mass due to the temperature-induced stimulation of SMA, can be expressed as follows:

$$\begin{aligned} N^r &= \iint_{A_w} [\varepsilon_0 - \alpha_s (T - T_0)] E_s dA_w = \\ &\sigma^r h_s V_s \end{aligned} \quad (19)$$

Where,  $E_s$ ,  $\alpha_s$ ,  $A_w$ ,  $h_s$ ,  $V_s$ ,  $T_0$ , and  $T$  are, respectively, the modulus of elasticity, thermal expansion coefficient, cross-sectional area, and thickness of the SMA-containing lamina, the volume fraction of SMA, the reference temperature, and the ambient temperature, and  $\varepsilon_0$  is the SMA pre-strain. The effect of SMA on the system can be modeled by applying the force  $N^r$  to the

system energy and integrating the resultants terms with respect to components and collecting the coefficients.

## 2.5. Solution of Equations

Adding an SMA-containing attached mass to the plate makes the Navier solution method inapplicable. Therefore, this study uses the Galerkin method. To solve the equations of motion, they must be transformed into displacement coefficients. This can be done by applying “Eqs. (1), (3) and (9)” to the equations of motion. In this study, boundary conditions are considered to be of the simply supported type. The next step is to apply the equations resulting from boundary conditions to the equations of motion in terms of displacement coefficients. Then, the shape functions of the equations must be multiplied by their respective equation of motion and then integrated over the area of the plate. Ultimately, this results in the equations to appear in the form of the following matrix:

$$\{[A] - \omega^2[B]\}\{C\} = \{0\} \quad (20)$$

Where,  $\{C\}$  is the displacement vector obtained by collecting the coefficients in the previous step, when they are sorted in ascending order.  $[A]$  is the stiff matrix and  $[B]$  is the mass matrix.

## 3 NUMERICAL RESULTS AND DISCUSSION

A program is developed in MATLAB to facilitate calculations. The validity and novelty of the approach are investigated by studying the instances of plate vibration problems in the existing literature. In some cases, the programs based on the FSDT and CLPT formulations are also used to better illustrate the accuracy of the present theory.

### 3.1. Validation

#### 3.1.1. The nondimensionalized natural frequencies for three plate thickness-to-side ratios

The main plate is considered to be a simply supported square composite plate with (0/90)s orthogonal stacking and the specifications given in “Table 1”.

**Table 1** Specifications of the main plate

$E_1/E_2=25$	$E_2=E_3$	$G_{12}=G_{13}=0.5E_2$	$G_{23}=0.2E_2$	$\nu_{12}=0.25$
--------------	-----------	------------------------	-----------------	-----------------

Attached to the main plate is a distributed mass with the specifications given in “Table 2”. The attached mass is isotropic and placed at the center of the plate.

**Table 2** Specifications of the attached mas

$E_a=E_2$	$\nu=0.33$	$c=0.2a$	$d=0.2a$	$\rho_a h_a=10\rho h$
$\Delta T = (T - T_0) = 100$ , $\varepsilon_0 = 1\%$ , $V_s = 0.1$				

“Table 3” shows the nondimensionalized natural frequencies of the described system for three plate thickness-to-side ratios. The nondimensionalization factor is considered to be as follows:

$$\bar{\omega} = \omega \left( \frac{a\rho}{E_2 h^2} \right)^{1/2}$$

The results reported in “Table 3” are for four states: (i) the plate without the distributed attached mass, (ii) the plate with the distributed attached mass but without the effect of the stiffness of the attached mass and SMA was considered, (iii) the plate with the distributed attached mass with only the effect of stiffness of the attached mass (not SMA) was considered, and (iv) the plate with the distributed attached mass with the effect of stiffness of the attached mass and SMA both was considered. The results obtained in this section are validated against the results of Malekzadeh et al. )K.Malekzadeh, S.Tafazoli, S.M.R.Khalili, 2010(. As shown in “Table 3”, the maximum difference between the results of the present work and those of )K.Malekzadeh, S.Tafazoli, S.M.R.Khalili, 2010 (is approximately 0.5%, which can be caused by the approximations or differences in the modeling procedure. Nevertheless, it can be claimed that the computed results have a good accuracy.

**Table 3** Nondimensionalized natural frequencies of the composite plate for three plate thickness-to-side ratios in four states

h/a	Source	1 <sup>st</sup> case	2 <sup>nd</sup> case	3 <sup>rd</sup> case	4 <sup>rd</sup> case
0.01	HOST [15]	15.1381	9.5775	12.6385	---
	Present	15.1078	9.5526	12.6252	12.9545
0.1	HOST [15]	11.7131	7.4333	9.7923	---
	Present	11.6756	7.3263	9.7469	10.0371
0.25	HOST [15]	7.1798	4.5153	5.8102	---
	Present	7.1466	4.4906	5.7916	5.9554

As “Table 3” indicates, incorporation of the effect of the attached mass can have a significant impact on the dynamic responses of the system. For example, in the solutions listed in the first row ( $h/a = 0.01$ ), ignoring this effect, by itself, results in about 32.2% difference in the responses. Regarding the impact of the presence of SMA in the attached mass, it can be seen that depending on the specifications of SMA, it can increase the frequency of the system. As shown in the third and fourth states, the presence of SMA with stated specifications improve the dynamic performance of the system by approximately 2.8%. Overall, these differences indicate the importance of incorporation of

the effect of the stiffness of the attached mass and SMA for obtaining high-quality results.

**3.1.2. The effect of ratios of elasticity moduli of the distributed attached mass to plate on the natural frequencies of the system with respect to various h/a ratios**

In this section, we investigate the effects of the elasticity modulus of the SMA-containing attached mass. In this example, the specifications are the same as given in “Tables 1 and 2”, and the nondimensionalization factor

$$\bar{\omega} = \omega \left( \frac{a\rho}{E_2 h^2} \right)^{1/2}.$$

To investigate the exclusive impact of the stiffness of the attached mass, we consider the first moment of mass. Although the used higher-order theory has 7 moment of mass terms, its dominant term is the first moment of mass. The natural frequency values obtained for different elasticity modulus and thickness ratios are presented in “Table 4”. For validation, these results are compared with the results provided in (K.Malekzadeh, S.Tafazoli, S.M.R.Khalili, 2010). The elastic modulus of the attached mass can be increased not only by changing the structure but also by adding the effect of SMA. In “Tables 3 and 4”, this effect is applied. The slight difference (maximum 3%) between these results and the results provided in (K.Malekzadeh, S.Tafazoli, S.M.R.Khalili, 2010) is due to the effect of SMA on the system. It should, however, be noted that the magnitude of this effect may vary with the characteristics of the SMA embedded.

**Table 4** Nondimensionalized natural frequencies of the composite plate for different elastic modulus and thickness ratios

h/a	Source	$E_a/E_1=1$	$E_a/E_1=2$	$E_a/E_1=4$	$E_a/E_1=6$
0.01	HOST [15]	12.6385	14.9224	18.3182	20.8310
	Present	12.9626	15.3286	18.8323	21.3752
0.1	HOST [15]	9.7923	11.6001	14.3722	16.4985
	Present	10.0693	11.9140	14.7546	16.9426
0.25	HOST [15]	5.8102	6.8222	8.3978	9.6237
	Present	5.9606	7.0052	8.6320	9.9003

As can be seen, increasing the elastic modulus and using SMA both increase the stiffness of the distributed attached mass, thereby increasing the natural frequencies of the system. The results listed in “Table 4” are plotted in “Fig. 3”. As illustrated in this plot, the changes in the elastic modulus of the distributed attached

mass cause incremental changes in the fundamental frequencies of the system. Moreover, the slope of the lines plotted in “Fig. 3” indicate that the stiffness of the attached mass has a more pronounced effect on thick plates than on thin plates.

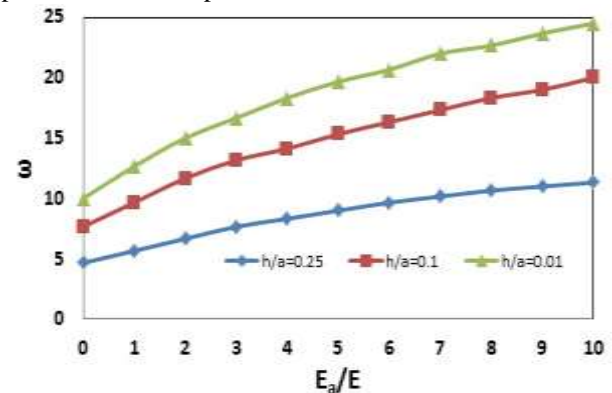


**Fig. 2** The effect of ratios of elasticity moduli of the distributed attached mass to plate on the natural frequencies.

**3.1.3. Effect of the ratio of distributed attached mass height to plate thickness for two plate thickness-to-side ratios**

This section discusses the effect of the ratio of mass height to plate thickness for different plate thicknesses-to-side ratios for the case where mass and plate have the same elastic modulus ( $E_a/E_1=1$ ). The system is assumed to have the same specifications as the system analyzed in Section (3.1.1) and a constant first moment of mass. The results obtained for different ratios of mass height to plate thickness and plate thicknesses-to-side ratios are given in “Table 5”. The results obtained in this section are validated against the results of Malekzadeh et al. (K.Malekzadeh, S.Tafazoli, S.M.R.Khalili, 2010). As before, the nondimensionalization factor is considered to

$$\bar{\omega} = \omega \left( \frac{a\rho}{E_2 h^2} \right)^{1/2}.$$

**Table 5** Nondimensionalized natural frequencies of the composite plate for different ratios of distributed attached mass height to plate thickness and plate thicknesses-to-side ratios

h/a	Source	$h_a/h=0.1$	$h_a/h=0.2$	$h_a/h=0.4$	$h_a/h=0.6$
0.01	HOST [15]	12.6385	14.8805	18.0544	20.1403
	Present	12.9089	15.4504	18.8704	21.3487
0.1	HOST [15]	9.7923	11.5641	14.1222	15.8111
	Present	9.9587	11.7954	14.4753	16.3803

With the first moment of mass assumed constant, increasing the thickness results in increased stiffness of the attached mass and consequently increased natural frequency of the system. As can be seen, the maximum

difference between these results and the ones provided in [15] is 7.1%, which is mostly due to the presence of SMA in the system. The greatest deviation in the results is seen in the case with  $ha/h=0.8$ , where the greater thickness of the attached mass leads to the increased effect of SMA due to its association with the alloy's volume fraction.

**3.1.4. Isotropic plate carrying a distributed attached mass without stiffness effect**

This section is dedicated to the validation of the results obtained in the present work against the results of Kopmaz et al. [12] and Malekzadeh et al. [15] for a simply supported isotropic plate with a distributed attached mass at its center. To prevent inconsistency with the above references and make the results comparable, the effect of the stiffness of the attached mass is ignored. Properties and dimensions of the main plate and the attached mass are given in “Tables 6 and 7”.

**Table 6** Specifications of the main plate

$E_1/E_2=25$	$E_2=E_3$	$a/h=0.01$	$b=1.5a$
--------------	-----------	------------	----------

**Table 7** Specifications of the attached mass

$E_a=E_2$	$\nu=0.33$	$c=0.1a$	$d=0.15a$	$\rho_a h_a=10\rho h$
-----------	------------	----------	-----------	-----------------------

$$\Delta T = (T - T_0) = 100 \quad , \quad \varepsilon_0 = 1\% \quad , \quad V_s = 0.1$$

In these tables,  $a$  and  $b$  are the width and length of the plate, the subscript  $a$  represents the attached mass,  $\rho$  is the density and  $h$  is the thickness of the plate,  $c$  and  $d$  are the width and length of the attached mass, and  $D$  is the flexural strength of the plate, which is defined as follows:

$$D = \frac{Eh^3}{12(1 - \nu^2)}$$

Where,  $E$  and  $\nu$  are the elastic modulus and the Poisson's ratio of the plate, respectively. The nondimensionalized form of the first four natural frequencies obtained in this work and the results given in [15] and [12] for isotropic plates with the attached mass are listed in “Table 8”. Here, the nondimensionalization factor is considered to be  $\bar{\omega} = \omega \left(\frac{D}{\rho a^4}\right)^{-1/2}$ .

As can be seen, the obtained results have a good consistency with the results of cited references, and their maximum difference remains below 5%. This difference is caused by the difference in how the inertia of the attached mass is analyzed and also the effect of SMA. From the above comparisons, it can be concluded that the adopted method is of acceptable precision, and can, therefore, be used for more extensive analysis in the search for novel and interesting results.

**Table 8** Non-dimensional frequencies of a simply-supported isotropic plate carrying a distributed mass on the width of the original plate

Present Method		Malekzade [15]	Kopmaz [12]
With SMA	Without SMA		
13.0088	12.7039	12.6785	12.0092
29.0665	28.5273	28.3854	27.2403
48.7589	47.5697	47.2860	43.2103
61.6909	59.9057	59.7623	56.9853

**3.2. Novel Results**

**3.2.1. Effect of temperature**

Given the temperature dependent variations in SMA's properties and recovery force that it applies to the lamina, the properties of the lamina embedded with SMA (Nickel.Titanium: NiTiNOL) wires may significantly vary with the temperature. Therefore, here we assess the dynamic behavior of a simply supported composite plate with SMA-containing (smart) attached mass in response to the changes in the temperature. The laminate stacking, geometric, and stiffness properties of the plate are given in “Tables 9 and 10”. Here, SMA is assumed to be embedded in the middle lamina of the attached mass and along the  $x$ -axis.

**Table 9** Specifications of the composite plate

Modulus of elasticity	Shear modulus	angles	Poisson's ratio	Dimensionless coefficient
$E_1/E_2=25$ $E_2=E_3$	$G_{12}=G_{13}=0.5E_2$ $G_{23}=0.5E_2$	$(0^\circ/90^\circ)_s$	$\nu_{12}=0.2$ 5	$=\bar{\omega}$ $(\rho E_2)^{1/2}/h$

**Table 10** Specifications of the distributed attached mass

Modulus of elasticity	Poisson's ratio	Dimensions of attached mass	Density	Dimensions of the main sheet
$E=E_1$ (of panel)	$\nu=0.33$	$c=0.2a$ $d=0.2b$	$\rho_a h_a = 10\rho h$	$a=2, b=1$

In “Fig. 4”, the variations in the natural frequencies of the SMA-containing system with the specifications listed in “Tables 9 and 10” are plotted in terms of variations in the SMA temperature. In “Fig. 5”, the first natural frequency of the system is plotted against the temperature of Nitinol. As can be seen, the increase in the temperature of SMA wires leads to an increase in the

natural frequency of the system. The first reason behind this association is that according to the aforementioned APT technique, the stiffness of SMA increases proportionally to temperature. Depending on the volume fraction of SMA wires, this stiffening leads to a degree of increase in the stiffness of the attached mass, and thus an increase in the overall frequency of the system. However, this stiffening makes at most 2% contribution to the increase in the natural frequency. The second cause lies in the ASET technique, since depending on the temperature and pre-strain of Nitinol wires, a compressive recovery stress will be applied and stiffen the structure. This phenomenon can also improve other dynamic behaviors of the structure. The results regarding the first natural frequency indicate its dependence on the temperature of SMA and the corresponding recovery stress. In this diagram (“Fig. 5”), the behavior of the natural frequency of the system in response to temperature variations of SMA is illustrated. Here, one can clearly see that as the recovery stress increase, so does the natural frequency of the system. Therefore, it is possible to control the system vibration by controlling the temperature applied to the SMA component. This diagram also indicates that the highest rate of increase in this frequency occurs in the temperature range of the inverse martensitic transformation in SMA.

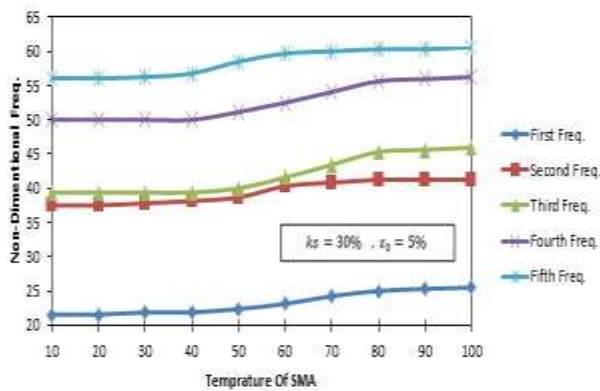


Fig. 4 Variations in the first five frequencies of the composite plate with a smart attached mass in term of variations in the SMA temperature.

Figure 6 shows the relative changes of the first five natural frequencies of the system with the specification listed in “Tables 9 and 10” in terms of variations in SMA temperature. In this diagram,  $\bar{\omega}_n$  denotes the natural frequencies of the system when the SMA is not stimulated, and  $\omega_n$  denotes the frequencies obtained with the effects of SMA stimulation considered. This figure also shows that the greatest change in the natural frequency occurs in the range of inverse martensitic transformation start and finish temperature. These results show that as temperature increases, SMA exhibits

a stronger positive impact on the frequencies, but on some frequencies - the fifth frequency ( $\omega_5$ ) for example – the effect is not desirable.

From the design perspective, it is interesting that the use of SMA in the attached mass most strongly affect the third frequency ( $\omega_3$ ), and the temperature increase leads to increased transverse stiffness of the structure. Overall, it can be stated that for the use of SMA to yield desirable results, system temperature should be raised above the temperature of martensitic transformation, otherwise the weight of the alloy will reduce the frequency of the system.

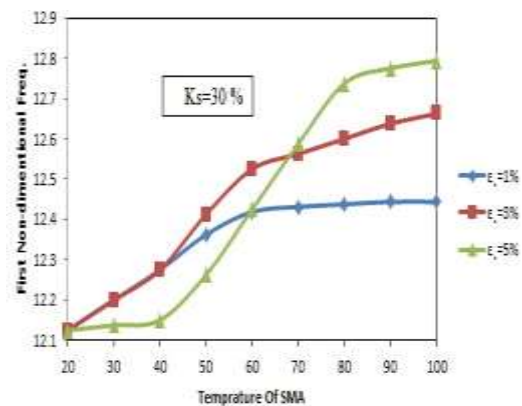


Fig. 5 Variations of the plate’s first natural frequency in terms of temperature for different SMA pre-strains.

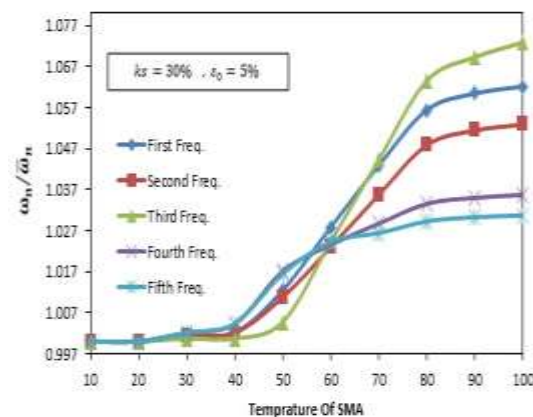


Fig. 6 The ratio of the first five frequencies of the plate with smart attached mass to the same frequencies without the stimulation of SMA in terms of SMA temperature.

### 3.2.2. Effect of the smart attached mass location

Here, we investigate the dynamical behavior of the simply supported composite plate in terms of the location of the attached mass. The stacking and geometric and stiffness properties of SMA are given “Tables 11, 12 and 13”. As before, SMA wires are assumed to be embedded in the middle lamina of the attached mass along the x-axis.

**Table 11** Specifications of the composite plate

Modulus of elasticity	Shear modulus	angles	Poisson's ratio	Dimensionless coefficient
$E_1/E_2=25$ $E_2=E_3$	$G_{12}=G_{13}=.05E_2$ $G_{23}=.02E_2$	$(0^\circ/90^\circ)_s$	$\nu_{12}=0.$ 25	$=\bar{\omega}$ $a^2 (\rho E_2)^{1/2} / h$

**Table 12** Specifications of the distributed attached mass

Modulus of elasticity	Poisson's ratio	Dimensions of attached mass	Density	Dimensions of the main sheet
$E=El$ (of panel)	$\nu=0.33$	$c=0.2a$ $d=0.2b$	$\rho_a h_a$ $= 10\rho h$	$a=2,$ $b=1$

**Table 13** Specifications of SMA

$Ks = 10 \%$	$\epsilon. = 5\%$
$\Delta T = 100$	

Figure 7 shows the variations in the first five natural frequencies of the smart system in terms of the position of the attached mass on the diameter of the original plate. Note that all dimensions discussed in this section are dimensionless. As can be seen, the first natural frequency has reached a minimum at the point (0.4a, 0.2b); these results could be of use for the design of the structure. Another notable result observed in “Fig. 7” is the unique behavior of the third frequency of the system.

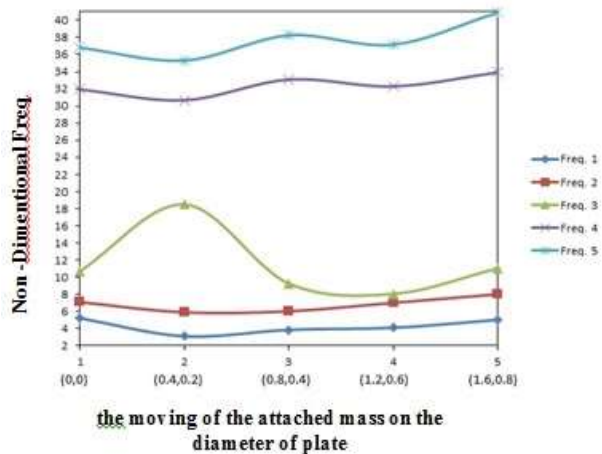


**Fig. 7** Variations in the first five natural frequencies of the system in terms of the position of the attached mass on the diameter of the original plate.

In “Fig. 8”, the first five natural frequencies of the smart system are plotted in terms of the position of the attached mass on the length of the plate (from the transverse perspective, the attached mass is positioned at the middle of the plate).

As can be seen, the fourth and fifth frequencies have relatively large variations that cannot be neglected. Again, the third frequency exhibits an interesting behavior, especially when the attached mass is placed in

the middle of the plate. The observed variations can be of great use for the system and facilitate more desirable behavior. The other interesting observation made in this diagram is that the first frequency behaves symmetrically relative to the center of the plate. As can be seen, the first frequency is smallest when the attached mass is positioned between the center of the plate and the support.

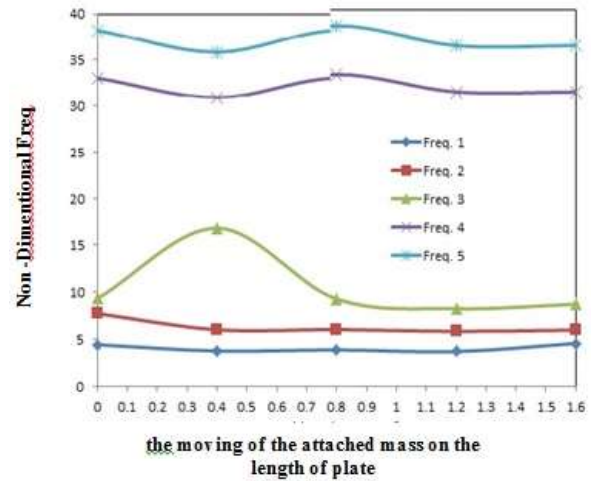


**Fig. 8** Variations in the first five natural frequencies of the system in terms of the position of the attached mass on the length of the original plate.

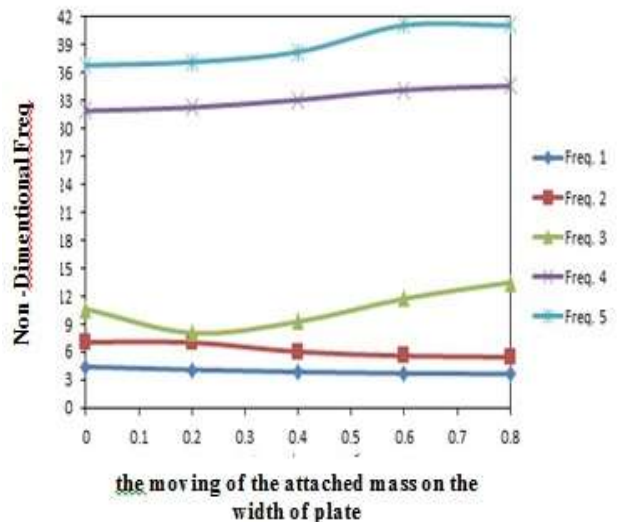


**Fig. 9** Variations in the first five natural frequencies of the system in terms of the position of the attached mass on the width of the original plate.

Figure 9 shows the variations of the first five natural frequencies of the smart system in terms of the position of the attached mass on the width of the plate (from the longitudinal perspective, the attached mass is positioned at the middle of the plate). As can be seen, the third frequency again exhibits an interesting behavior. The

almost completely uniform behavior of the first frequency across the spectrum is also notable. The third interesting observation is the lower variations of frequencies in this chart as compared to others.

**3.2.3. Effect of SMA pre-strain**

This section examines the effects of SMA pre-strain on the system frequencies. The specifications of the system in this section are given in “Tables 11 and 12”. In “Fig. 10”, the effects of different SMA pre-strain on frequency variations are plotted in terms of SMA volume fraction. It can be seen that, at the temperature of 100°C (the inverse transformation finish temperature), as the SMA volume fraction increases, the first, second and fifth natural frequencies of the system increase. This effect is more pronounced in larger pre-strains. In other words, the larger is the pre-strain, the greater is the effect of volume fraction on the first five frequencies.

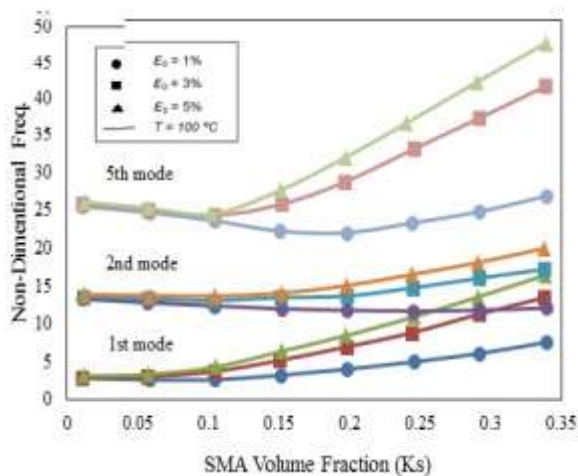


Fig. 10 Effect of SMA pre-strain on the natural frequencies in terms of SMA volume fraction.

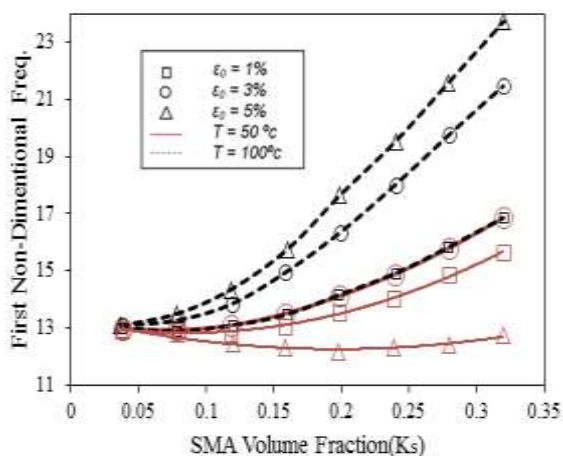


Fig. 11 Effect of SMA pre-strain on the natural frequencies in terms of Nitinol volume fraction at 50°C and 100°C.

Figure 11 illustrates the variations in natural vibrations of the system with the specifications of “Tables 11 and 12” and with different SMA pre-strains and volume fractions at two different temperatures. As mentioned earlier, as the SMA volume fraction increases, the temperature-dependent tensile recovery stress of fibers leads to an increase in the geometric stiffness of the system and thus an increase in its natural frequency. This figure also shows that at 50°C, 3% SMA pre-strain has the greatest impact on the natural vibration of the system. This is clearly because SMA has the greatest recovery stress at 50°C and 3% pre-strain.

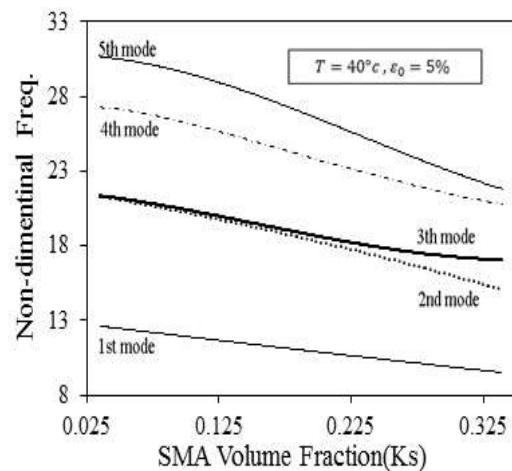


Fig. 12 Effect of volume fraction of Nitinol fibers on the first five frequencies of the system at 40°C.

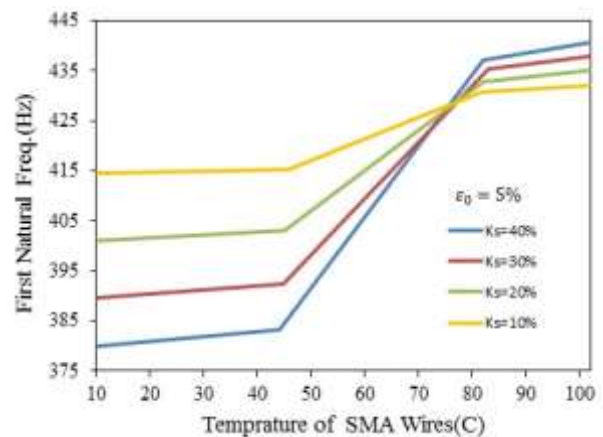


Fig. 13 Effect of SMA volume fraction on the variations of first natural frequency in terms of SMA temperature.

**3.2.4. Effect of SMA volume fraction**

The following diagrams illustrate the effects of SMA volume fraction on the system frequency for different SMA pre-strains. As before, these diagrams are plotted for the system with the specifications given in “Tables 11 and 12”. Figure 12 shows that for the pre-strain of  $\epsilon_0 = 5\%$  and at the temperature of 40°C (below the

martensitic transformation finish temperature), as the volume fraction of Nitinol fibers increases, the first five natural frequencies of the system decrease. This inverse relation can be attributed to the increase in the mass of the system.

As shown in “Fig. 13”, the higher is the volume fraction, the further affected is the natural frequency. In other words, it is possible to somewhat control the system frequencies by controlling the volume fraction of SMA fibers. In “Fig. 13”, there is a turning point for the system vibrations, where all volume fractions have the same effect. At the temperature below this point, larger volume fractions lead to increasing frequency reduction, but at a higher temperature, larger volume fractions increase the system frequency.

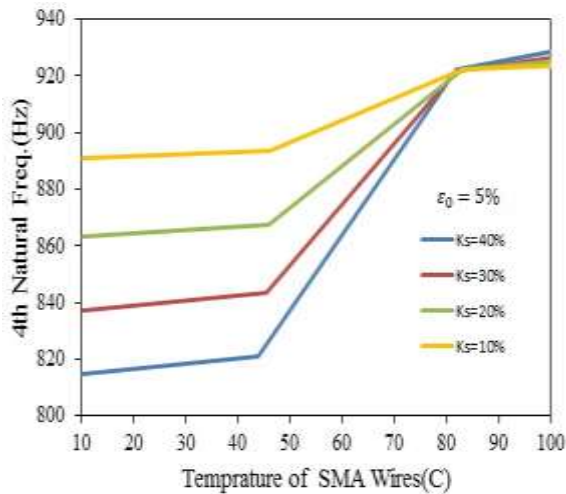


Fig. 14 Effect of SMA volume fraction on the variations of the fourth natural frequency in terms of SMA temperature.

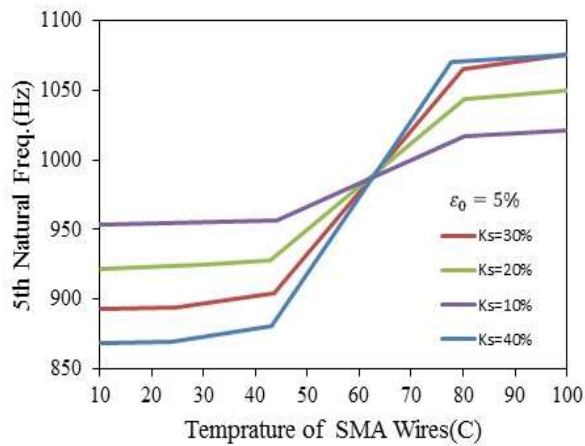


Fig. 15 Effect of SMA volume fraction on the variations of the fifth natural frequency in terms of SMA temperature.

According to “Figs. 13, 14 and 15”, before the completion of transformation phase, an increase in the SMA volume fraction reduces the natural frequency, but beyond the transformation finish temperature, the

increase in volume fraction increases the frequency of the system. This is because before the completion of inverse transformation (at temperatures below the austenite phase finish temperature), the increased weight of the structure overshadows the increased SMA recovery stress due to increased Nitinol content, thus leading to a reduction in the frequency of the system.

However, at a higher temperature, this compressive stress (Nitinol recovery stress) dominates the effects of weight gain, resulting in an increase in the frequency of the system. It should be reiterated that how the smart systems with different SMA pre-strains and volume fraction behave directly depends on the temperature of SMA wires. In other words, the dynamic behaviors of the system below the transformation temperature after the start of transformation are different. This is due to compressive recovery stress of the SMA fibers, which, once the transformation initiates, starts to stiffen the system.

**3.2.5. Effect of SMA and attached mass on the order and shapes the system modes**

Here, we examine the effect of smart attached mass on the mode shapes of the system with the specifications given in “Tables 11, 12 and 13”, which undergo some changes following the variations in the system parameters. Here, the investigation is limited to the mode shapes of the system with smart attached mass with the stiffness of the attached mass considered.

Given the specifications of the system in question the use of Galerkin method for analysis, it is possible to obtain the mode shapes in term of approximation parameters *m* and *n*. The mode shapes and order obtained for the system with given specifications and different *m* and *n* values are listed in “Table 14”.

Table 14 Order of the natural frequencies of the system for different *m* and *n* values

Natural Fre.	n	m	arrangement
0.8597	3	3	1
1.0993	2	3	2
2.5712	3	2	3
3.5271	1	3	4
3.5381	3	1	5
3.5649	2	1	6
3.5764	2	2	7
3.5926	1	2	8
3.8704	1	1	9

As shown in the “Table 14”, the lowest natural frequency is obtained in the case where *m* and *n* are both 3. Although, according to “Table 14”, the order of

natural frequencies and their relation to different  $m$  and  $n$  values does not follow a predictable trend. For example, as shown in “Table 14”, the natural frequency obtained with  $m = 1$  and  $n = 2$  is lower than the one obtained with  $m = 2$  and  $n = 2$ , but it cannot be stated that for the higher the  $m$  and  $n$  values, the natural

frequency will not be necessarily lower. Therefore, when solving such problems, the choice of optimal  $m$  and  $n$  values is very important for the determination of mode shapes. To gain a better understanding of the issue, the mode shapes obtained for the above nine states are plotted in “Fig. 16”.

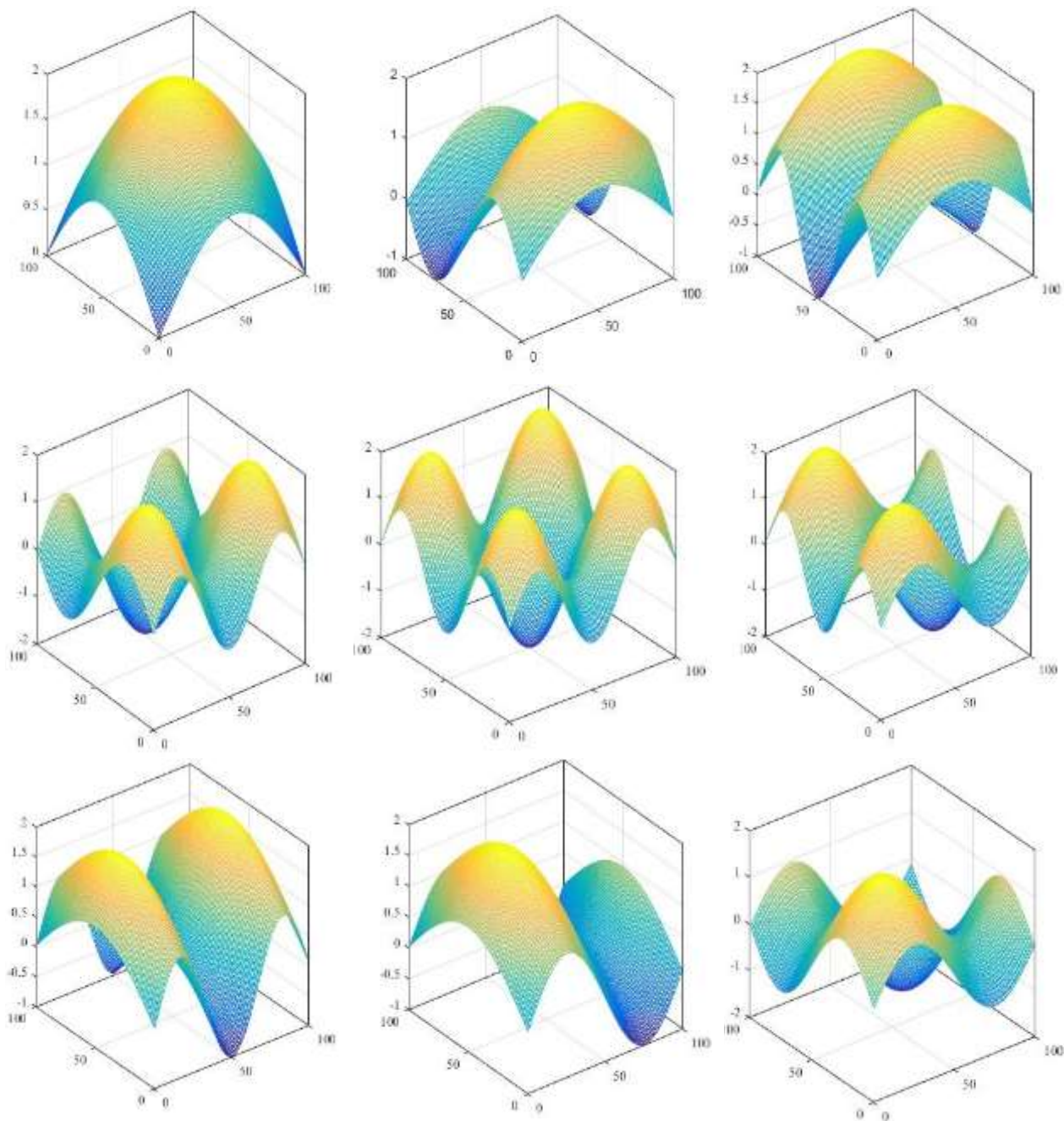


**Fig. 16** The mode shape obtained with different  $m$  and  $n$  values.

---

#### 4 CONCLUSION

---

The results obtained in this study can be summarized as follows:

- Examination of the effect of the thickness of the distributed attached mass showed that with the first moment of mass considered constant, as this thickness increases so does the natural frequency of the system. In other words, a thicker attached mass leads to higher stiffness.
- Even with the effect of SMA ignored, the addition of the attached mass alters the natural frequencies of the system. There is an inverse relationship between the mass inertia of the attached mass and the natural frequencies, and a direct relationship between the stiffness of the attached mass and the natural frequencies of the system.
- Dimensions of the distributed attached mass can affect the natural frequencies of the entire system. Using a thicker attached mass results in an increase in both the mass inertia and the stiffness.
- With the effect of the stiffness of the attached mass ignored, the addition of the mass to the composite plate increases the plate deflection by an amount that depends on the density.
- Stimulation of SMA fibers has a positive effect on the increase in natural frequencies.
- The best rate of increase in the natural frequency due to the heating of SMA fibers was seen in the range of inverse transformation temperatures.
- Addition of SMA fibers without increasing the temperature reduces the natural frequencies.
- At a constant temperature below the transformation start temperature, increasing the SMA volume fraction increases the density of the attached mass and thus the transverse deformation of the plate.
- At a given temperature, increasing the SMA pre-strain increases the recovery stress, which results in an increase in the natural frequencies.
- The system where the attached mass is positioned in the middle of the plate, does not necessarily have the lowest frequency.
- The best rate of increase in the frequency occurs in the system where the attached mass is located above one of the supports.
- The third frequency has an almost unpredictable behavior, which requires special attention from the designer.
- When the attached mass was moved along the length of the plate, the changes in the first frequency exhibited symmetry relative to the center of the plate.
- Incorporation of the parameters such as the frequencies into the choice of optimal values for the parameters  $m$  and  $n$  is of significant importance for the determination of mode shapes of the system.

---

#### 5 REFERENCES

---

- [1] Yang, P. C., Norris, C. H., and Stavsky, Y., Elastic Wave Propagation in Heterogeneous Plates, International Journal of Solids and Structures, Vol. 2, No. 4, 1966, pp. 665-684.
- [2] Kant, T., Owen, D. R. J., and Zienkiewicz, O. C., A Refined Higher Order C0 Plate Bending Element, Computers & Structures, Vol. 15, No. 2, 1982, pp. 177-183.
- [3] Reddy, J. N., A Simple Higher-order Theory for Laminated Composites, ASME Journal of Applied Mechanics, Vol. 51, No. 4, 1984, pp. 745-752.
- [4] Reddy, J. N., Phan, N. D., Stability and Vibration of Isotropic, Orthotropic and Laminated Plates According to a Higher-order Shear Deformation Theory, Journal of Sound and Vibration, Vol. 98, No. 2, 1985, pp. 157-170.
- [5] Khdeir, A. A., Free Vibration and Buckling of Symmetric Cross-ply Laminated Plates by an Exact Method, Journal of Sound and Vibration, Vol. 126, No. 3, 1988, pp. 447-461.
- [6] Khdeir, A. A., Free Vibration and Buckling of Unsymmetric Cross-ply Laminated Plates Using a Refined Theory, Journal of Sound and Vibration, Vol. 128, No. 3, 1989, pp. 377-395.
- [7] Qatu, M. S., Recent Research Advances in the Dynamic Behavior of Shells:1989-2000, Part 1: Laminated Composite Shells, Applied Mechanics Reviews, Vol. 55, No. 4, 2002, pp. 325-350.
- [8] Qatu, M. S., Recent Research Advances in the Dynamic Behavior of Shells:1989-2000, Part 2: Homogeneous Shells, Applied Mechanics Reviews, Vol. 55, No. 5, 2002, pp. 415-434.
- [9] Garg, A. K., Khare, R. K., and Kant, T., Higher-order Closed-form Solutions for Free Vibration of Laminated Composite and Sandwich Shells, Sandwich Structures and Materials, Vol. 8, No. 3, 2006, pp. 205-235.
- [10] Gorman D. J, Singal R. K., Analytical and Experimental Study of Vibrating Rectangular Plates On Rigid Point Supports, AIAA Journal, Vol. 29, No. 5, 1991, pp. 838-844.
- [11] Rossi, R. E., A. Laura, P. A., Symmetric and Antisymmetric Normal Modes of a Cantilever Rectangular Plate: Effect of Poisson's Ratio and A Concentrated Mass, Journal of Sound and Vibration, Vol. 195, No. 1, 1996, pp. 142-148.
- [12] Kopmaz, O., Telli, S., Free Vibration of a Rectangular Plate Carrying Distributed Mass, Journal of Sound Vibration, Vol. 25, No. 1, 2002, pp. 39-57.
- [13] Wong, W. O., The Effect of Distributed Mass Loading On Plate Vibration Behaviour, Journal of Sound and Vibration, Vol. 252, No. 3, 2002, pp. 577-583.
- [14] Alibeiglooa, A., Shakeri, M., Kari, and M. R., Free Vibration Analysis of Antisymmetric Laminated Rectangular Plates with Distributed Patch Mass Using

- Third-Order Shear Deformation Theory, *Ocean Engineering*, Vol. 35, No. 2, 2008, pp. 183-190.
- [15] Malekzadeh, K., Tafazoli, S., and Khalili, S. M. R., Free Vibrations of Thick Rectangular Composite Plate with Uniformly Distributed Attached Mass Including Stiffness Effect, *Journal of Composite Materials*, Vol. 44, No. 24, 2010, pp. 2897-2918.
- [16] Ostachowicz, W., Krawczuk, M., and Zak, A., Dynamic and Buckling of a Multilayer Composite Plate with Embedded SMA Wires, *Composite Structures*, Vol. 48, No. 1-3, 2000, pp. 163-167.
- [17] Lau, K. T., Zhou, L. M., and Tao, X. M., Control of Natural Frequencies of a Clamped-Clamped Composite Beam with Embedded Shape Memory Alloy Wires, *Composite Structures*, Vol. 58, No. 1, 2002, pp. 39-47.
- [18] Mozafari, A., Malekzadeh, K., Ahmadi, M., and Azarnia, A. H., Analyze of Free Vibration of Composite Plate with Embedded Shape Memory Alloy, in *ISME16*, Kerman, 2008.
- [19] Zhang, R. X., Ni, Q. Q., Masuda, A., Yamamura, T., and Iwamoto, M., Vibration Characteristics of Laminated Composite Plates with Embedded Shape Memory Alloys, *Composite Structures*, Vol. 74, No. 4, 2006, pp. 389-398.
- [20] Park, J. S., Kim, J. H., and Moon, S. H., Vibration of Thermally Post-Buckled Composite Plates Embedded with Shape Memory Alloy Fibers, *Composite Structures*, Vol. 63, No. 2, 2004, pp. 179-188.
- [21] Ni, Q. Q., Zhang, R. X., Natsuki, T., and Iwamoto, M., Stiffness and Vibration Characteristics of SMA/Er3 Composites with Shape Memory Alloy Short Fibers, *Composite Structures*, Vol. 79, No. 4, 2007, pp. 501-507.
- [22] Zhang, Y., Zhao, Y. P., A Study of Composite Beam with Shape Memory Alloy Arbitrarily Embedded Under Thermal and Mechanical Loadings, *Materials and Design*, Vol. 28, No. 4, 2007, pp. 1096-1115.
- [23] John, S., Hariri, M., Effect of Shape Memory Alloy Actuation On the Dynamic Resposns of Polymeric Composite Plates, *Composites Part A: Applied Science and Manufacturing*, Vol. 39, No. 5, 2008, pp. 769-776.
- [24] Shokuhfar, A., Khalili, S. M. R., Ashenai Ghasemi, F., Malekzadeh, K., and Raissi, S., Analysis and Optimization of Smart Hybrid Composite Plates Subjected to Low-Velocity Impact Using the Response Surface Methodology (RSM), *Thin-Walled Structures*, Vol. 46, No. 11, 2008, pp. 1204-1212.
- [25] Ibrahim, H. H., Yoo, H. H., and Lee, K. S., Aero-Thermo-Mechanical Characteristics of Imperfact Shap Memory Alloy Hybrid Composite Panels, *Journal o Sound and Vibration*, Vol. 325, No. 3, 2009, pp. 583-596.
- [26] Kuo, S. Y., Shiau, L. C., and Chen, K. H., Buckling Analysis of Shape Memory Alloy Reinforced Composite Laminates, *Composite Structures*, Vol. 90, No. 2, 2009, pp. 188-195.
- [27] Malekzadeha, K., Mozafari, A., and Ashenai Ghasemi, F., Free Vibration Response of a Multilayer Smart Hybrid Composite Plate with Embedded SMA Wires, *Solids and Structures*, Vol. 11, No. 2, 2014, pp. 279 - 298.
- [28] Sadd, M. H., *Elasticity: Theory and Applications*, Second Edition, 1993.
- [29] Reddy, J. N., *Mechanics of Laminated Composite Plates and Shells*, 2nd Edition, CRC Press, 2004.